The University of Tehran Press

Pollution

Print ISSN: 2383-451X
Online ISSN: 2383-4501

https://jpoll.ut.ac.ir/

Impact of Fertilizer Factory Emissions on Radiological Content of Soil: A Study in Upper Egypt

Soad Saad Fares[1, 2]✉

1. Departments of Physics, Faculty of Science, Baha University, Saudi Arabia
2. Department of Radiation Physics, National Center of Radiation Research and Technology NCRRT, Atomic Energy Authority, Cairo, Egypt.

Article Info

Article type:
Research Article

Article history:
Received: 14 January 2024
Revised: 13 March 2024
Accepted: 06 May 2024

Keywords:
Upper Egypt
Soil
Internal hazard External hazard Radium equivalent

ABSTRACT

This study investigated the potential impact of a fertilizer factory in Upper Egypt on the surrounding soil's radioactivity levels. Gamma-ray spectrometry was used to measure the concentrations of naturally occurring radionuclides (^{226}Ra, ^{232}Th, and ^{40}K) in soil samples collected near the factory. Additionally, radon gas concentrations were measured, and various radiological hazard indices were calculated. Activity concentrations of ^{238}U, ^{226}Ra, ^{232}Th, and ^{40}K varied in the soil samples, ranging from 110.63 to 326.12 Bq/kg for ^{238}U, 172.72 to 582.37 Bq/kg for ^{226}Ra, 25.63 to 189.15 Bq/kg for ^{232}Th, and 252.20 to 713.24 Bq/kg for ^{40}K. Radium equivalent activity, absorbed gamma dose, and external and internal hazard indices exceeded permissible levels. Radon gas concentrations varied from 20.89 to 192.30 Bq/m^3, with an average of 104.43 Bq/m^3. The calculated effective dose from radon inhalation exceeded the recommended limit. The elevated levels of radioactivity in soil and the high radon gas concentrations suggest a potential health risk for farmers and residents near the fertilizer factory. Further investigations and mitigation strategies may be necessary to ensure the safety of the surrounding population.

Cite this article: Fares S. S. (2024). Impact of Fertilizer Factory Emissions on Radiological Content of Soil: A Study in Upper Egypt. *Pollution*, 10 (2), 790-807.
https://doi.org/10.22059/poll.2024.371108.2222

© The Author(s). Publisher: The University of Tehran Press.
DOI: https://doi.org/10.22059/poll.2024.371108.2222

INTRODUCTION

Since the dawn of humanity, our connection with the environment has been fundamental to our existence. Initially, we lived as nomadic gatherers, relying directly on nature's bounty for survival. This "gathering stage" involved minimal manipulation of the environment, similar to herbivorous animals. However, as our cognitive abilities evolved through experience, we transitioned to a "pastoral stage" characterized by animal domestication and rudimentary agriculture. This shift demanded a deeper understanding of natural cycles and phenomena, leading to significant cultural and social advancements (McNeill, 2000). The current "industrial stage" marks a turning point in our relationship with the environment. We have become architects of our surroundings, manipulating the environment through heating, cooling, and harnessing power sources to suit our needs. This shift in control, as (Worster, 1994) argues, has placed the reins firmly in our hands. The phosphate fertilizer industry exemplifies the complex relationship between progress and environmental impact. While it plays a crucial role in modern agriculture, it also ranks among the most polluting chemical industries. Despite efforts to improve practices,

*Corresponding Author Email: *sfares2@yahoo.com*

challenges persist due to technological limitations and the industry's inherent complexity. The phosphate fertilizer industry exemplifies this complex dynamic. Though crucial for modern agriculture, it ranks among the most polluting chemical sectors due to its water treatment plants, power generation facilities, and boilers. Despite Egypt's efforts to improve environmental practices, challenges remain (Cordell, et al., 2019). First, advanced production technology often involves hazardous substances and generates significant waste, posing environmental risks. Second, the industry's reliance on fossil fuels contributes to greenhouse gas emissions and air pollution. Finally, improper waste disposal can lead to soil and groundwater contamination.

While indispensable for food production, the phosphate fertilizer industry faces a critical turning point. Striking a balance between progress and sustainability requires a multi-faceted approach (ICRP, 2017). Adopting cleaner production technologies, utilizing renewable energy sources, and implementing stricter environmental regulations are crucial steps towards ensuring a healthy future for both humanity and the environment. Today, we stand in the industrial age, where we have constructed our own artificial environment through advancements like heating, cooling systems, and harnessed power sources. This shift has fundamentally altered the relationship between humans and the environment. Once dictated by natural balance, we now hold the reins, shaping the world around us (Lutz, et al., 2017). However, this influence comes at a cost. The phosphate fertilizer industry, although vital for modern agriculture, exemplifies the complex challenges of industrial progress. Its operations, encompassing water treatment, power generation, and boilers, contribute significantly to environmental degradation. While efforts have been made in Egypt to improve environmental practices within this industry, several hurdles remain (UNEP, 2019). One major challenge lies in outdated technology, which often involves hazardous substances and generates substantial waste, posing significant environmental risks. Moving forward, navigating this complex relationship requires a delicate dance between progress and sustainability (Ahmed, 2005). By investing in cleaner production technologies, exploring renewable energy sources, and implementing stricter environmental regulations, we can strive for a future where humanity and the environment thrive together.

1. GEOLOGIC SETTING

The phosphate fertilizer factory is situated at coordinates 27°11′47”N, 31°6′59”E, approximately 9 kilometers north of Assiut city, Egypt (Figure 1.A & 1.B). Established in 1978, the factory boasts an installed capacity of 14,600 metric tons and a total plant capacity of 205,000 metric tons per year. Its strategic location between the western bank of the Nile River and (Mohamed, et al. 2013) navigation canal provides easy access to the main express roads of Assiut-Cairo, Assiut-Aswan, and the railway station. The region experiences prevailing northwesterly winds from November to March, transitioning to north-westerly to northerly winds for the remainder of the year. The soil composition is predominantly limestone-based, with textures ranging from sand to loamy sand (El-Taher, et al., 2013). The study area encompasses agricultural land both within and surrounding the Assiut fertilizer factory. Given that this soil supports crops consumed by humans and animals, it is crucial to investigate the concentrations of radionuclides present and assess the potential impact of the factory on these levels.

Additional coordinates:
Assiut city: 27°10′00”N, 31°11′00”E
Nile River: 28°59′23”N, 31°12′58”E
El-Ibraheimia navigation canal: 27°58′41”N, 31°13′55”E
Assiut-Cairo express road: 28°01′46”N, 31°12′44”E
Assiut-Aswan express road: 27°14′41”N, 31°11′05”E
Railway station: 27°11′23”N, 31°11′16”E

Fig. (1. A). Phosphate fertilizer factory in Assiut, Egypt, and its harmful emissions

Fig. (1. B). Phosphate fertilizer factory in Assiut, Egypt, and its harmful emissions

2. RADIOACTIVITY MEASUREMENTS

2.1. Radioactivity Analysis of Soil Samples

This study measured the activity concentrations of naturally occurring radionuclides in soil samples using high-resolution gamma-spectrometry (Figure 2A, 2B, 2C). A high-purity germanium (HPGe) detector with 70% efficiency) Produced by Canberra Company (was employed for this purpose (Figure 3C). Calibration of the system was achieved using certified reference materials with similar densities to the soil samples (IAEA, 2021). Measurements were conducted in a controlled laboratory environment at the Egyptian Ministry of Defense, with each sample analyzed for up to 90,000 seconds. The acquired spectra were then processed and analyzed using Canberra Genie 2000 software (version 3.0). Specific gamma-ray transitions were utilized to quantify the activity of different radionuclides: ^{238}U or ^{226}Ra: Determined from the 92.38 keV (5.6%) gamma-ray emission of its daughter nuclide, ^{234}Th (assuming radioactive equilibrium). ^{232}Th: Estimated using the gamma-ray energies of ^{212}Pb (238.6 keV, 45%), ^{228}Ac (338.4 keV, 12.3%), 911.07 keV (29%), and 968.90 keV (17%). ^{40}K: Directly measured using its own 1460.8 keV (10.7%) gamma-ray emission. Due to its low abundance (0.72% of total uranium), ^{235}U was excluded from this analysis. Background radiation levels were determined by measuring an empty polystyrene container using the same method. These values were subsequently subtracted from the measured sample values to obtain accurate activity concentrations. Additionally, the decay daughters of the radionuclides were measured to confirm the activity concentrations (Majeed, et al., 2014). The intensity of each gamma-ray line was carefully measured and corrected for

Fig. (2-A). One of the fertilizer factory's products is phosphate fertilizer

Fig. (2-B). Sample packed in MARINELLI beaker

Fig. (2-C). HPGe detector system

various factors like sample mass, branching ratios, counting time, and detector efficiency to ensure reliable activity quantification. In summary, this study employed a high-resolution HPGe gamma-spectrometry system with appropriate calibration and analysis techniques to accurately determine the activity concentrations of ^{238}U, ^{226}Ra, ^{232}Th, and ^{40}K in soil samples (Majeed, et al., 2014).

2.2. CR-39 detectors

CR-39 detectors are solid-state nuclear track detectors that are commonly used to measure radon gas concentrations. They are made of a polymer material that is sensitive to alpha particles, which are emitted by radon gas. When an alpha particle hits the detector, it creates a track that can be visualized and counted using a microscope. The sealed cup technique is a method for measuring radon gas concentrations in soil and other samples using CR-39 detectors. The

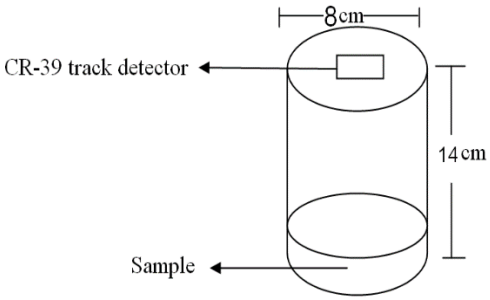

Fig. 3. A schematic diagram of the sealed-cup technique in soil sample

sample is placed in a sealed container and the radon gas is allowed to accumulate for a period of time, typically 25 days. The CR-39 detector is then placed in the container and the radon gas is allowed to etch the detector. The number of tracks on the detector is proportional to the concentration of radon gas in the sample. CR-39 detectors are a reliable and accurate method for measuring radon gas concentrations. They are also relatively inexpensive and easy to use. However, they are not without their limitations. For example, CR-39 detectors can be affected by temperature and humidity, and they can also be susceptible to interference from other alpha-emitting isotopes (Mohammad, et al., 2012) (Figure 3).

2.3. Activity Concentration Determination

The activity concentrations of the samples were then calculated using the following equation1 (IAEA, 2015) (Figure 4).

$$C\ (Bq/kg) = Cn * (1/\varepsilon * t * m) * (1/P\gamma) \quad (1)$$

Where: C is the activity concentration of the radionuclide (Bq/kg), Cn is the net count under the photopeak of the gamma ray, ε is the detector efficiency for the gamma ray, t is the counting time (seconds), m is the mass of the sample (kg) and Pγ is the abundance of the gamma ray. For ^{226}Ra and ^{232}Th, the following equations were used to calculate the activity concentrations from the decay daughters (Al-Masri, et al., 2005):

$$C(^{226}Ra) = (N / t * m * e) \quad (2)$$

and

$$C(^{232}Th) = (C / I * Eff * M * Bg) \quad (3)$$

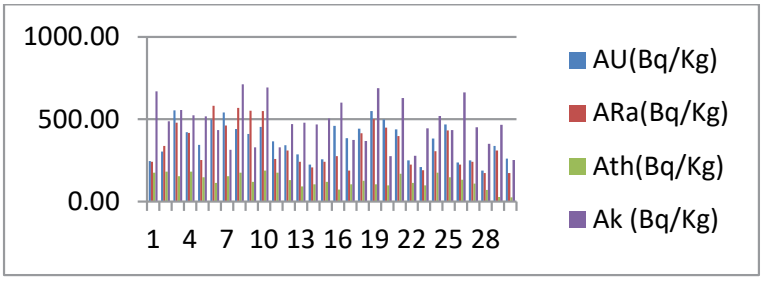

Fig. 4. Activity concentration from ^{238}U, ^{226}Ra, ^{232}Th and ^{40}K element

Where: C is the activity concentration in (Bq/kg), N is the net counts in the peak of interest, t is the counting time in seconds, m is the mass of the sample in kilograms, (IAEA, 2022) e is the detector efficiency at the energy of the peak of interest, C is the CSP_{net}, I is the internal conversion coefficient, E_{ff} is the efficiency of the detector for the energy of the gamma ray, M is the mass of the sample and Bg Background counts in the same region of interest (usually in cps). These equations were used to calculate the activity concentrations of ^{238}U, ^{226}Ra, ^{232}Th, and ^{40}K in each sample.

3. RADIOLOGICAL HAZARD INDICES

3.1. Absorbed and Effective Dose Rate (D)

The absorbed dose rates due to gamma radiation in the air at one meter above the ground surface were calculated using the following formulas (IAEA, 2021) (Figure 5):

$$D = 0.462C_{Ra} + 0.604C_{Th} + 0.0417C_{K} \quad (4)$$

where D is the absorbed dose rate in air (nGy/h), and C_{Ra}, C_{Th}, and C_K are the activity concentrations (IAEA, 2018) of ^{226}Ra, ^{232}Th, and ^{40}K in Bq/kg, respectively.

The annual effective dose rate (mSv/y) was calculated using the following formula:

$$(mSv/y) = D \times 24\ hours \times 365.25\ days \times 0.2 \times 0.7\ Sv/Gy \times 0.001 \quad (5)$$

The exposure rate was calcolat using the Equation (6).

$$E_R\ (\mu Rh^{-1}) = 1.90\ C_{Ra} + 2.82\ C_{Th} + 0.179\ C_K \quad (6)$$

The absorbed dose rate in air due to gamma radiation from the naturally occurring radionuclides ^{226}Ra, ^{232}Th, and ^{40}K can be calculated using these equations (UNSCEAR, 2008) Additional Equations:

$$D\ (pGy\ s^{-1}) = 8.69\ E\ (\mu R\ h^{-1}) * 3.6\ Gy\ s^{-1} / \mu R\ h^{-1} = 31.28\ E\ (pGy\ s^{-1}) \quad (7)$$

$$D\ (mSv\ y^{-1}) = 0.0833\ E\ (\mu R\ h^{-1}) * 31.5360\ x\ 10\text{^}6\ \ mSv\ y^{-1} / \mu R\ h^{-1} = 2628\ E\ (mSv\ y^{-1}) \quad (8)$$

Using these equations, the absorbed dose rate in air (D), annual effective dose rate (mSv/y),

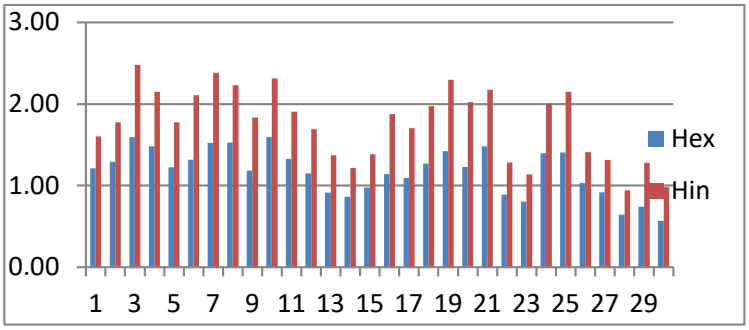

Fig. 5. External hazard index (H_{ex}) and internal (Hin) hazard index

and exposure rate (E) can be calculated from the activity concentrations of ^{226}Ra, ^{232}Th, and ^{40}K. (ICRU, 1996).

3.2. Radium Equivalent: Assessing Gamma Radiation Hazard in Materials.

The radium equivalent (Ra_{eq}) serves as a crucial index for estimating the combined gamma radiation dose arising from naturally occurring radionuclides like ^{226}Ra, ^{232}Th, and ^{40}K. This calculation, expressed as

$$Ra_{eq} = C_{Ra} + 1.43\ C_{Th} + 0.077\ C_K \quad (9)$$

Where C represents the activity concentrations of each isotope in Becquerels per kilogram (Bq/kg), enables the comparison of radioactivity across samples containing different combinations of these radionuclides. The importance of this index stems from the potential health risks associated with prolonged exposure to gamma radiation. Organizations like the World Health Organization (WHO, 2021) and the United Nations Scientific Committee on the Effects of Atomic Radiation (UNSCEAR, 2000) have emphasized the significance of Raeq in mitigating these risks through informed material selection and radiation protection practices.

3.3. External Hazard Index: Gauging Radiation Risk from Natural Sources

The external hazard index (H_{ex}) provides a crucial metric for gauging the external radiation exposure humans face from naturally occurring radionuclides. This widely used index, expressed as:

$$H_{ex} = (C_{Ra} + 1.43\ C_{Th} + 0.077\ C_K) / 370 \quad (10)$$

Considers the activity concentrations of Radium (Ra), Thorium (Th), and Potassium (K) series respectively (Bq/kg). A value less than 1 indicates negligible radiation hazard, highlighting its role in evaluating potential health risks. Emphasizing its relevance for building materials and other naturally occurring radionuclide sources (IAEA, 2021). Prolonged exposure to gamma radiation can pose health risks like increased cancer risk. Thus, the Hex facilitates comparisons between materials, enabling informed choices for construction and other applications. In conclusion, the Hex serves as a powerful tool for evaluating the external radiation hazard associated with materials and environments harboring naturally occurring radionuclides (Beretka, et al., 1985).

3.4. Internal Hazard Index: Assessing Internal Radon Exposure

The internal hazard index (H_{in}) plays a crucial role in estimating the internal radiation exposure humans receive from radon and its short-lived decay products. This established metric, expressed as

$$H_{in} = (C_{Ra} + 0.7\ C_{Th} + 0.3\ C_K) / 185 \quad (11)$$

Considers the activity concentrations of Radium (Ra), Thorium (Th), and Potassium (K) series (Bq/kg). Its primary function lies in evaluating potential health risks associated with radon exposure. This standardized index assesses the internal radiation hazard posed by materials or environments by accounting for the potential radon production from these major naturally occurring radionuclides. A Hin value less than 1 suggests negligible internal radiation risk, highlighting its relevance for building materials and other naturally occurring radionuclide sources. Prolonged exposure to radon can significantly increase the risk of lung cancer (WHO, 2021).

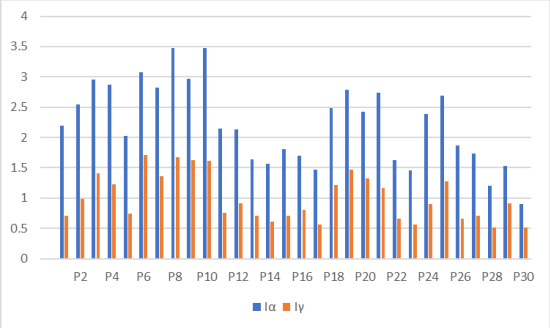

Fig. 6. Representative level index Iγ, Iα

3.5. Representative Level Index: Assessing Overall Radiation Hazard.

The representative level index (Iγr) serves as a valuable indicator of the combined radiation hazard posed by naturally occurring radionuclides like ^{226}Ra, ^{232}Th, and ^{40}K. This widely used index, expressed as (Figure 6)

$$I_{\gamma r} = (C_{Ra}/150 + C_{Th}/100 + C_K/1500) < 1 \quad (12)$$

By comparing each radionuclide's concentration to reference values and summing the results, the Iγr provides a standardized assessment of radiation risk. These reference values ensure that a material with Iγr of 1 would pose the same gamma radiation dose as a specific combination of Ra, Th, and K. This index proves valuable for comparing the radiation hazard of various materials like soil, building components, and environmental samples. It also helps assess potential risks from natural radiation exposure. Essentially, the Iγr considers the combined gamma dose from these major natural contributors, offering a comprehensive perspective on overall radiation hazard.

3.6. Alpha Representative Level Index: Gauging Indoor Radon Risk.

The alpha representative level index (Iαr) gauges the potential radiation hazard of inhaling radon gas emitted from building materials. This widely used index relies on the formula

$$I_{\alpha r} = C_{Ra} / 200 \leq 1 \quad (13)$$

where C_{Ra} represents the activity concentration of ^{226}Ra in the material (Bq/kg). Essentially, Iαr indicates the alpha radiation risk relative to a limit of 200 Bq/kg of ^{226}Ra. Values less than 1 suggest negligible concern, making it valuable for identifying materials and buildings potentially susceptible to high radon levels. By directly assessing the alpha radiation hazard posed by building materials, Iαr plays a crucial role in: Evaluating potential health risks: Prolonged exposure to radon, primarily an alpha emitter, increases lung cancer risk. Iαr allows comparisons between materials, minimizing health risks.

4. RADON GAS MEASUREMENT

4.1. Assessing Radon Risk Around a Phosphate Fertilizer Factory

Radon exhalation rate (RER), measured in Becquerels per square meter per day (Bq/m^2·day), signifies the amount of radon gas released from soil. It's crucial for evaluating health risks associated with radon exposure. CR-39 detectors, solid-state nuclear track detectors, were used in a study by (Mohamed, et al., 2013) to measure RER in soil samples collected near a phosphate

fertilizer factory (Hesham, et al., 2016).

$$HE\ (mSv\ y^{-1}) = C\ x\ F\ x\ T\ x\ D \quad (14)$$

Where: C is the radon concentration in the air (Bq/m^3), F is the occupancy factor (0.4), T is the time spent indoors (hours per year) and D is the dose conversion factor for radon gas. The study revealed RER values ranging from 13.92×10^{-6} to 81.82×10^{-6} Bq/m^2·day, with an average of 45.19×10^{-6} Bq/m^2·day. The highest value was found within the factory itself. Additionally, a positive correlation was observed between RER and radium content, as radium decays into radon. The annual effective dose (HE) for the public due to radon exposure was calculated using the provided equation, considering factors like radon concentration, occupancy, indoor time, and dose conversion factor. Worryingly, the study found HE values exceeding the internationally permissible limit of 10 mSv/year for residents near the factory, indicating a significant health risk.

4.2. Assessing Radon Exhalation Near a Phosphate Fertilizer Factory

Radon, a radioactive gas originating from the decay of naturally occurring soil and rock radium, poses a lung cancer risk when inhaled. Studying its release rate is crucial for evaluating potential health hazards. A study by (Mohammad, et al., 2013) investigated radon exhalation from soil samples collected near a phosphate fertilizer factory. They measured both the mass exhalation rate (amount of radon released per unit mass of soil per unit time) and the surface exhalation rate (amount released per unit area per unit time). The study found average mass and surface exhalation rates ranging from 1.78 to 10.46 Bq/kg and 13.92 x 10^{-6} to 81.82 x 10^{-6} Bq/m^2·day^{-1}, respectively, with overall averages of 5.78 Bq/kg and 45.19 x 10^{-6} Bq/m^2·day^{-1}. Radon exhalation mass rates varied from 20.92 x 10^{-8} to 122.94 x 10^{-8} Bq/kg·day^{-1}, averaging 67.90 x 10^{-8} Bq/kg·day^{-1}. While none of the samples exceeded the international limit of 35 pCi/L (NCRP, 2009), it's essential to remember that even minimal exposure carries a non-zero lung cancer risk. Interestingly, the study revealed a positive correlation between radium content and radon exhalation rate, supporting the link between radium decay and radon production. Notably, samples closest to the factory exhibited the highest exhalation rates.

4.3. Strong Correlation Between ^{238}U Activity and Mass Exhalation

This section explores the significant relationship between uranium-238 (^{238}U) activity concentration and mass exhalation. A highly positive and statistically significant correlation exists between these two variables. The fitted model, expressed as:

$$Mass\ exhalation\ *10^{-8} = 0.000159918 + 0.239184^{*}\ C_U \quad (15)$$

(where CU represents ^{238}U activity concentration), explains all data variations with an R-squared value of 100% (NCRP, 2014). Furthermore, the model exhibits accuracy with a low standard error of the residual (0.00283724) and a small absolute error value (0.00242825). Additionally, the P-value for serial autocorrelation exceeds 0.05, indicating no significant serial dependence in the residuals at the 95% confidence level. This implies that the residuals are independent, confirming the lack of a pattern and solidifying the direct relationship between ^{238}U content and its exhaled amount. In simpler terms, as the amount of ^{238}U in the body increases, so does the amount exhale (UNSCEAR, 2008). This statistically significant relationship suggests it's unlikely due to chance, making the model valuable for predicting exhaled ^{238}U based on its body content. Scientific.

4.4. Strong Positive Correlation Between ^{226}Ra and ^{238}U Activity Concentrations

This section analyzes the relationship between the activity concentrations of radium-226 (^{226}Ra) and uranium-238 (^{238}U), revealing a statistically significant and positive correlation. The fitted model:

$$C_{Ra} = 2.43438 + 5.28092 * C_U \quad (16)$$

CRa aligns with a strong correlation coefficient of 0.9269, suggesting a clear positive association. This value indicates a trend approaching perfect positive correlation (1) and exceeding chance occurrence (P-value < 0.05) (UNSCEAR, 2008). Furthermore, the model explains 92.694% of the data variance, highlighting a good fit. However, caution regarding potential overfitting is necessary. Standard deviation (30.0613) and mean absolute error (MAE, 22.4122) provide insights into data variability and model accuracy. A lower standard deviation indicates less data scatter, and a lower MAE suggests better model predictions. The absence of significant serial autocorrelation (P-value > 0.05) implies independent residuals and confirms no underlying patterns in the data, strengthening the observed relationship (ICR, 2017). Possible Explanations: Natural Co-occurrence: ^{226}Ra and ^{238}U often exist together in nature, like uranium ores. Mining and processing activities can release both into the environment, potentially exposing people nearby. This study demonstrates a strong and significant positive correlation between ^{226}Ra and ^{238}U activity concentrations.

4.5. Strong, Positive Correlation Between ^{238}U Activity and Surface Radon Release

Analysis of the relationship between surface radon release (Bq/kg·day^{-1}) and the activity concentration of uranium-238 (^{238}U) revealed a statistically significant and positive correlation at the 95% confidence level. The fitted model:

$$Surface\ exhalation\ *10^{-6} = 2.43438 + 5.28092 * CU \quad (17)$$

With an R-squared value of 1.0, suggests a perfect fit to the data. However, potential overfitting is worth considering. The observed correlation coefficient of 1.0 indicates a perfect positive relationship, meaning both variables increase linearly together. While rare in real-world data, it signifies a strong association. Regarding model accuracy, a low standard deviation (0.00283724) and absolute error (0.00242825) suggest good performance (NCRP, 2014). Additionally, the absence of significant serial autocorrelation (P-value > 0.05) confirms independent residuals and strengthens the observed relationship. Possible Explanations: Natural Co-occurrence: Similar to previous sections, 238U and radon often co-exist in nature, like uranium ores. Mining and processing activities releasing both elements can potentially expose nearby populations (WNA, 2022).

5. RESULTS AND DISCUSSION

5.1. Environmental Pollution and Increased Radiation Due to Phosphate Fertilizer Factory Dust

This study investigated environmental pollution caused by dust emissions from a phosphate fertilizer factory, focusing on its impact on radiation levels in the surrounding area. Key Findings: Activity concentrations of naturally occurring radionuclides (^{226}Ra, ^{238}U, ^{232}Th, and ^{40}K) were detected in all soil samples (Table 1), ranging from 172.72 Bq/kg to 713.24 Bq/kg. Average activity concentrations were 340.33 Bq/kg for ^{226}Ra, 126.56 Bq/kg for 238U, 106.56 Bq/kg for ^{232}Th, and 476.48 Bq/kg for ^{40}K. Spatial Variation: Radionuclide concentrations increased with proximity to the factory, following the order: $^{232}Th < {}^{40}K < {}^{238}U < {}^{226}Ra$. Elevated Levels:

Concentrations of ^{238}U and ^{226}Ra exceeded permissible limits set by (UNSCEAR, 2008) in all samples. Implications: Dust emissions from the factory contribute to environmental pollution, potentially impacting surrounding communities. Elevated levels of ^{238}U and ^{226}Ra raise concerns about potential health risks associated with long-term exposure (Ahmed, 2005).

5.2. Absorbed Dose and Potential Health Risks

Analyzed Soil Samples Show Elevated Radiation Levels, But Not Immediate Health Risk. This

Table 1. Activity concentration from ^{238}U, ^{226}Ra, ^{232}Th and ^{40}K, Radium equivalent (Ra_{eq}) and External hazard index (H_{ex}) and internal (H_{in}) hazard index

Sample	A_U (Bq/Kg)	A_{Ra} (Bq/Kg)	A_{Th} (Bq/Kg)	A_K (Bq/Kg)	Ra_{eq} (Bq/Kg)	H_{ex}	H_{in}
P1	144.79	242.19	176.00	668.84	545.37	1.21	1.60
P2	179.07	337.37	182.57	486.76	635.93	1.29	1.77
P3	326.13	479.77	154.80	555.68	743.92	1.59	2.48
P4	247.45	417.01	182.50	524.00	718.34	1.48	2.15
P5	202.86	252.74	147.41	518.23	503.44	1.23	1.77
P6	293.17	582.37	112.31	434.19	776.41	1.32	2.11
P7	318.11	462.11	154.43	314.08	707.13	1.52	2.38
P8	259.53	569.97	175.48	713.24	875.83	1.53	2.23
P9	241.46	552.69	119.33	328.79	748.65	1.18	1.83
P10	266.19	550.58	189.15	693.32	874.45	1.59	2.31
P11	214.64	258.19	175.48	329.16	534.48	1.33	1.91
P12	200.94	310.89	131.15	471.50	534.74	1.15	1.69
P13	168.88	241.10	92.73	479.70	410.63	0.91	1.37
P14	132.07	207.26	105.29	469.21	393.95	0.86	1.22
P15	151.26	241.80	119.70	504.22	451.80	0.98	1.38
P16	271.13	276.52	73.52	601.55	427.97	1.14	1.87
P17	225.89	189.23	104.92	374.90	368.13	1.09	1.70
P18	260.76	414.52	126.35	367.69	623.51	1.27	1.97
P19	322.85	500.88	105.29	689.83	704.56	1.42	2.30
P20	293.51	449.06	98.27	276.41	610.87	1.23	2.02
P21	257.63	397.63	168.98	629.56	687.74	1.48	2.18
P22	146.75	224.53	112.31	279.00	406.62	0.89	1.28
P23	123.05	189.99	98.27	444.69	364.76	0.80	1.14
P24	225.55	306.67	175.48	520.66	597.70	1.40	2.00
P25	275.44	431.79	147.78	434.19	676.55	1.41	2.15
P26	139.97	224.53	133.37	663.52	466.34	1.03	1.41
P27	146.89	242.03	110.09	451.69	434.24	0.92	1.31
P28	110.63	172.72	70.19	350.15	300.06	0.64	0.94
P29	198.79	311.06	28.08	467.38	387.20	0.74	1.28
P30	153.59	172.72	25.63	252.20	228.78	0.57	0.98
S.D	**64.87**	**131.55**	**43.51**	**133.32**	**170.19**	**0.29**	**0.44**
Avg.	**216.63**	**340.33**	**126.56**	**476.48**	**558.00**	**1.17**	**1.76**
Min	**110.63**	**172.72**	**25.63**	**252.20**	**228.78**	**0.57**	**0.94**
Max	**326.13**	**582.37**	**189.15**	**713.24**	**875.83**	**1.59**	**2.48**

section analyzes the absorbed dose rates and annual effective doses associated with the radioactive elements found in the soil samples. Key findings: Absorbed dose: Ranged from 61.08 to 232.52 nGy/hour, averaging 147.75 nGy/hour, exceeding the normal range (18-93 nGy/hour) and the average (59 nGy/hour) (Table 2). Annual effective dose (external): Estimated at 0.07 to 0.29 mSv/year, averaging 0.18 mSv/year, staying below the global permissible limit (0.480 mSv/year). Internal effective dose: Calculated as 0.30 mSv/year, 1.14 mSv/year, and 0.72 mSv/year, all below the international limit of 1 mSv/year. While soil samples show contamination with radioactive elements, current levels don't pose immediate health risks. Monitoring contamination levels

Table 2. I_{α}, I_{γ} and Absorbed dose rate

Sample	I_{α}	I_{γ}	D(nGy|\h)	Deff (AEDE) outdoor(mSv/y)	Deff (AEDE) indoor(mSv/y)	ELCR (indoor)
P1	2.19	0.71	142.79	0.18	0.70	2.88
P2	2.54	0.99	167.60	0.21	0.82	3.39
P3	2.96	1.41	197.46	0.24	0.97	3.26
P4	2.87	1.23	189.93	0.23	0.93	2.27
P5	2.02	0.74	132.36	0.16	0.65	3.56
P6	3.08	1.71	207.52	0.25	1.02	3.23
P7	2.82	1.36	187.95	0.23	0.92	3.99
P8	3.48	1.68	232.52	0.29	1.14	3.43
P9	2.97	1.63	200.02	0.25	0.98	3.98
P10	3.48	1.62	231.87	0.28	1.14	2.41
P11	2.14	0.76	140.51	0.17	0.69	2.43
P12	2.13	0.91	141.33	0.17	0.69	1.86
P13	1.64	0.71	108.49	0.13	0.53	1.78
P14	1.57	0.61	103.68	0.13	0.51	2.04
P15	1.81	0.71	119.00	0.15	0.58	1.95
P16	1.70	0.81	113.41	0.14	0.56	1.66
P17	1.47	0.56	96.86	0.12	0.48	2.85
P18	2.48	1.22	165.78	0.20	0.81	3.22
P19	2.79	1.47	187.66	0.23	0.92	2.80
P20	2.42	1.32	163.18	0.20	0.80	3.12
P21	2.74	1.17	181.72	0.22	0.89	1.84
P22	1.63	0.66	107.33	0.13	0.53	1.65
P23	1.46	0.56	95.96	0.12	0.47	2.70
P24	2.39	0.90	157.31	0.19	0.77	3.08
P25	2.69	1.27	179.56	0.22	0.88	2.10
P26	1.87	0.66	122.32	0.15	0.60	1.97
P27	1.73	0.71	114.55	0.14	0.56	1.36
P28	1.20	0.51	79.22	0.10	0.39	1.78
P29	1.53	0.91	103.65	0.13	0.51	1.05
P30	0.90	0.51	61.08	0.07	0.30	1.05
S.D	**0.68**	**0.39**	**45.45**	**0.06**	**0.22**	**0.83**
Avg.	**2.22**	**1.00**	**147.75**	**0.18**	**0.72**	**2.49**
Min	**0.9**	**0.51**	**61.08**	**0.07**	**0.3**	**1.05**
Max	**3.48**	**1.71**	**232.52**	**0.29**	**1.14**	**3.99**

over time remains crucial to ensure their stability. Samples near the factory (P3, P4, P6, P7, P8, P9, P19) suggest the factory as a potential source (Yanagisawa, et al. 1992).

5.3. Non-Uniform Radioactivity Distribution and Potential Health Risks

This section analyzes the Radium Equivalent (Ra_{eq}) and External Hazard Index (H_{ex}) of the soil samples (Table 1), focusing on their spatial variation and potential health implications. Key Findings: Ra_{eq}: Values ranged from 228.78 to 875.83 Bq/kg, exceeding the permissible limit of 370 Bq/kg (UNSCEAR, 2008). The highest Raeq was found near the factory (P3), decreasing with distance. H_{ex}: Average values ranged from 0.57 to 1.59, with some exceeding the international limit. Samples near the factory (P3 to P9) displayed higher H_{ex} values compared to distant locations (P30). Overall soil samples closer to the factory exhibit higher radioactivity and external hazard indices, suggesting potential health risks (Abbady, 2006).

5.4. Gamma Exposure, Alpha Risk Factors, and Potential Cancer Risk

This section examines gamma exposure values (Iγ), alpha risk factors (Iα), and their implications for potential cancer risk (Table 2). Key Findings: Gamma Exposure (Iγ): Values ranged from 0.51 to 1.71, with higher values near the factory (P3). Samples closer to the factory (P3-P25) had Iγ exceeding 1, while others (P11, P17, P5) remained below 1. Alpha Risk Factors (Iα): All samples exceeded the permissible limit for ^{238}U (Iα > 1), indicating potential alpha radiation risks. Excess Lifetime Cancer Risk (ELCR): Calculated values ranged from $1.05x10^{-3}$ to $3.99x10^{-3}$, exceeding the global average of $0.29x10^{-3}$. This suggests an elevated cancer risk for individuals residing or working near the factory. Overall soil samples closer to the factory exhibit higher radioactivity, external hazard indices, and ELCR values, suggesting a potential increase in cancer risk for nearby populations.

5.5. Radon Exhalation and Potential Health Risks

This section analyzes the radon exhalation rates in soil and air samples, along with their implications for potential health risks (Table 3). Key Findings: Exhalation Rates: Average mass and surface exhalation rates in soil ranged from 6.60 Bq/kg to 60.73 Bq/m^3 (average 32.98 Bq/m^3). Air samples exhibited higher average values (20.89 Bq/kg to 192.30 Bq/m^3, average 104.43 Bq/m^3), and indoor samples displayed similar levels (23.06 Bq/kg to 194.47 Bq/m^3, average 106.60 Bq/m^3). Inhalation Dose: Calculated values ranged from 43.36 to 399.18 μSv/year (average 216.77 μSv/year). Effective Dose Rate: Values ranged from 0.73 to 6.13 mSv/year (average 3.36 mSv/year), exceeding the global permissible limit of 1 mSv/year for two samples (P29 and P30). Overall residents in the study area are exposed to higher radiation levels than the global average, likely due to naturally occurring radioactive elements in soil and rocks. The highest exhalation rate was found near the factory (sample P2). Radon gas levels in all samples remained below the international limit (35 pCi/L). A positive correlation exists between radium content and exhalation rate.

5.6. Correlations between Naturally Occurring Radionuclides

This section analyzes the relationships between naturally occurring radionuclides (^{226}Ra, ^{238}U, ^{232}Th, and ^{40}K) found in soil samples. Key Findings: Strong positive correlation (0.9963) between ^{226}Ra and ^{238}U suggests a common origin or closely related sources. Moderate positive correlation (0.789) between ^{232}Th and ^{40}K indicates a possible shared source or related sources. Weak or absent correlations between ^{238}U and ^{40}K, and ^{232}Th and ^{40}K, suggest distinct origins or differing mobility due to soil processes. Possible Explanations: Geological Formations: Diverse soil formations in the study area could contribute to variations in radionuclide levels.

Table 3. Measurement of radon nutrient produced from sand collected from and around the phosphate fertilizer plant

Sample	^{222}Rn in soil (Bq/m^3)	^{222}Rn in Air (Bq/m^3)	^{222}Rn in vegetabls (Bq/m3)	^{222}Rn indoor	Doses from inhalation gas (µsv/y)	HE (mSv y^{-1})
P1	43.59	138.05	244.12	140.22	286.55	4.42
P2	60.73	192.30	340.07	194.47	399.18	6.13
P3	39.85	126.18	223.13	128.35	261.91	4.05
P4	46.98	148.76	263.07	150.93	308.79	4.76
P5	37.94	120.15	212.48	122.32	249.41	3.86
P6	28.91	91.54	161.89	93.71	190.02	2.96
P7	39.75	125.87	222.59	128.04	261.28	4.04
P8	45.17	143.04	252.95	145.21	296.91	4.58
P9	30.72	97.26	172.01	99.44	201.90	3.14
P10	48.69	154.18	272.65	156.35	320.04	4.93
P11	45.17	143.04	252.95	145.21	296.91	4.58
P12	33.76	106.90	189.04	109.07	221.90	3.44
P13	23.87	75.58	133.66	77.75	156.89	2.45
P14	27.10	85.82	151.77	87.99	178.15	2.77
P15	30.81	97.57	172.54	99.74	202.53	3.15
P16	18.92	59.92	105.97	62.09	124.39	1.96
P17	27.01	85.52	151.23	87.69	177.52	2.77
P18	32.52	102.99	182.12	105.16	213.78	3.32
P19	27.10	85.82	151.77	87.99	178.15	2.77
P20	25.29	80.10	141.65	82.27	166.27	2.59
P21	43.49	137.73	243.57	139.90	285.90	4.41
P22	28.91	91.54	161.89	93.71	190.02	2.96
P23	25.29	80.10	141.65	82.27	166.27	2.59
P24	45.17	143.04	252.95	145.21	296.91	4.58
P25	38.04	120.45	213.01	122.62	250.04	3.87
P26	34.33	108.71	192.24	110.88	225.65	3.50
P27	28.34	89.73	158.69	91.90	186.27	2.90
P28	18.07	57.21	101.18	59.38	118.77	1.87
P29	7.23	22.89	40.47	25.06	47.51	0.79
P30	6.60	20.89	36.94	23.06	43.36	0.73
Min	**6.60**	**20.89**	**36.94**	**23.06**	**43.36**	**0.73**
Max	**60.73**	**192.30**	**340.07**	**194.47**	**399.18**	**6.13**
Avg.	**32.98**	**104.43**	**184.67**	**106.60**	**216.77**	**3.36**

Geological Minerals: Differences in geological minerals might explain variations between ^{238}U and ^{232}Th levels. Overall, the study reveals various correlations between radionuclides, suggesting potential shared origins or distinct sources based on their strength. These findings, along with the observed variability, are likely linked to the diverse geological makeup of the studied area, as previously reported in literature (Majeed, et al., 2014) (Figure 7).

5.7. Table (4) Explanation: Radioactivity Levels in Soil Samples

This table compares the radioactivity levels of ^{226}Ra, ^{232}Th, and ^{40}K in the studied soil samples

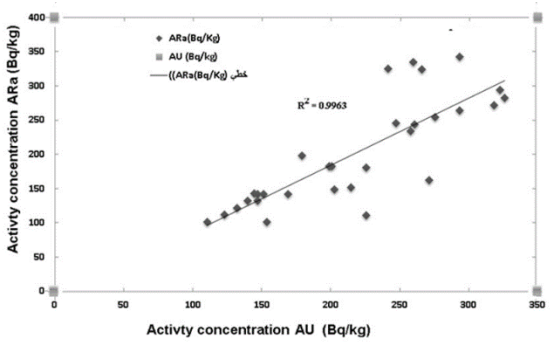

Fig. 7. Linear regression of the activity concentration of ^{238}U versus ^{226}Ra

Table 4. Comparison of radioactivity levels in soil samples under investigation with a similar study

Country	^{226}Ra	^{232}Th	^{40}K	Reference
Egypt	16.92	21.96	505.92	**Harb et al. (2014)**
Egypt	23.66	13.95	146.33	**Sroor et al. (2001)**
Egypt	31.12	10.96	264.1	**Nada et al. (2009)**
Pakistan	30-38	50-64	560-635	**Akhtar et al. (2005)**
India	46.52	54.81	543.43	**Golmakani et al. (2008)**
Turkey	85.75	51.08	771.57	**Ajithra et al. (2017)**
Algeria	53.2	50.03	311	**Becegato et al. (2008)**
Egypt	**340.33**	**126.56**	**476.48**	**Present work**

with those from other studies conducted in various countries. Country: Egypt (4 studies): Show varying levels of radioactivity across different Egyptian locations. Pakistan, India, Turkey and Algeri. Present work: Represents the average values from the current study in Egypt. Key Observations: The present study's ^{226}Ra and ^{40}K levels are higher than most other studies, while ^{232}Th levels are comparable. This suggests potentially elevated radiation levels in the studied Egyptian location compared to other regions. However, it's important to note: Direct comparisons are challenging due to differences in sampling methods, analysis techniques, and geological variations.

6. CONCLUSION

Environmental Impact and Public Health Concerns, this study raises critical concerns regarding the potential health risks associated with residing near a phosphate fertilizer factory due to elevated radiation exposure. Key Findings: Increased Radiation Exposure: Residents near the factory exhibited annual effective dose rates (AEDE) exceeding the permissible limit of 1 mSv, suggesting potential health risks from chronic exposure. External Radiation Hazard: Hex index values for samples near the factory (P3-P19) surpassed the international limit, indicating a heightened external radiation hazard. Radon Exhalation: Elevated radon gas levels, a known carcinogen, were detected in the study area, further amplifying health concerns. This study highlights the potential environmental impact of phosphate fertilizer factories and their associated public health risks. Further investigations and mitigation strategies are imperative to ensure the safety and well-being of communities residing near such facilities.

7. RECOMMENDATION

Monitoring: Continued monitoring of radioactivity levels is crucial to track any changes and ensure their stability. Source Investigation: Further investigation at the factory is necessary to pinpoint the source of contamination and implement mitigation strategies. Comprehensive Assessment: A broader assessment considering various factors beyond Raeq and Hex is crucial for a complete understanding of potential radiological hazards. This includes the type and energy of radiation, exposure duration, and individual risk factors. Comprehensive Assessment: A broader assessment, considering factors beyond Iγ and Iα, is crucial for accurately evaluating cancer risks. This includes internal exposure, individual risk factors, and specific types and energies of radiation. Mitigation Strategies: Based on a comprehensive assessment, implementing effective mitigation strategies to reduce radiation exposure and minimize potential health risks is essential. Resident Relocation: Considering the potential health risks, relocating residents living close to the factory is crucial to minimize their exposure. Emission Reduction: Implementing pollution control measures or modifying factory operations is essential to reduce the release of radioactive elements into the environment.

ACKNOWLEDGMENTS

The author would like to thank members of our Central lab, in National Center for Radiation Research and Technology NCRRT, Atomic Energy Authority, Cairo, Egypt in the preparation of this manuscript. The authors also thank the staff of laboratory chemical warfare, radioactive materials department, the Egyptian Ministry of Defense for the helpful and cooperated contribution in achieving this work.

GRANT SUPPORT DETAILS

The present research did not receive any financial support.

CONFLICT OF INTEREST

The authors declare that there is not any conflict of interests regarding the publication of this manuscript. In addition, the ethical issues, including plagiarism, informed consent, misconduct, data fabrication and/ or falsification, double publication and/or submission, and redundancy has been completely observed by the authors.

LIFE SCIENCE REPORTING

No life science threat was practiced in this research.

NOTES ON CONTRIBUTORS

Soad Fares: Prof. Dr. is a Senior Research Scientist of National Center for Radiation Research and Technology NCRRT, Atomic Energy Authority, Cairo, Egypt. She too now a Prof. Dr. in Department of Physics, Faculty of Science, Baha University, Saudi Arabia.

REFERENCES

Ahmed, NK. (2005). Measurement of natural radioactivity in building materials in Qena city, Upper Egypt. J Environ Radioact; 3: 91–99.

Ajithra, A.K., Venkatraman, B., Jose M.T., Chandrasekar, S., & Shanthi G. (2017). Assessment of natural radioactivity and associated radiation indices in soil samples from the high background radiation area, Kanyakumari district, Tamil Nadu, India. Radiat Protect Environ 40, 27.1. 27-33. https://inis.iaea.org/search/search.aspx?orig_q=RN:49058789

Akhtar, Nasim; Tufail, M; Ashraf, M & Mohsin Iqbal, M. (2005). Measurement of environmental radioactivity for estimation of radiation exposure from saline soil of Lahore, Pakistan. Iqbal, Ra Radiation Measurements 39, Issue 1, 11. doi:10.1016/j. radmeas.2004.02.016.

Allaby, M. (2012). A dictionary of environment and conservation. Oxford University Press.

Abbady, A. (2006). "Level of Natural Radionuclides in Foodstuffs and Resultant Annual Ingestion Radiation Dose," Nuclear Science and Techniques, Vo1. 17, No. 5, 2006, pp. 297-300.

Al-Masri, M. S., Jaradat, Q. M., & Hudaib, M. (2005). Natural radioactivity levels and dose assessment in building materials used in Jordan. Journal of Environmental Radioactivity, 81(2-3), 17-26.

Beretka, J, Mathew PJ. (1985). Natural radioactivity of Australian building materials, industrial wastes and by-products. Health Phys.;48(6):87-95.

Cordell, D., McGlade, J., White, S., & Valentin, L. (2019). Global phosphorus flows from production to consumption. Global Biogeochemical Cycles, 33(2), 170-205.

El-Taher, A. & Alharbi, A. (2013). Radioactivity levels and assessment of radiological hazards in phosphate fertilizers and associated rocks from Egypt. Life Science Journal, 10(2), 532-539.

Food and Agriculture Organization of the United Nations (FAO) & International Atomic Energy Agency (IAEA). (2022). Manual on the application of the FAO/WHO international standards for food and feed irradiation. Vienna, Austria: IAEA.

Golmakani, S. Ahabi Moghaddam, V. M. & Hosseini,T. (2008). "Factors Affecting the Transfer of Radionuclides from the Environment to Plants," Radiation Protection Dosimetry, Vol. 130, No. 3, pp. 1-8.

Harb, S., El-Kamel, A.H., Abd El-Mageed, A.I., Abbady, A. & Rashed, W. (2014). Radioactivity Levels and Soil-to-Plant Transfer Factor of Natural Radionuclides from Protectorate Area in Aswan, Egypt. World J Nucl Sci Technol 4, 7. doi:10.4236/wjnst.2014.41002.

Hesham, A., Yousef Gehad, M., Saleh, A.H., El-Farrash, A & Hamza, c. (2016). Radon exhalation rate for phosphate rocks samples using alpha track detectors. Volume 9, Issue 1, January, Pages 41-46.

ICRP, (1996). Publication 74, Conversion Coefficients for Use in Radiological Protection against External Radiation, Ann. ICRP 26(3/4).

International Atomic Energy Agency (IAEA). (2018). Technical Reports Series No. 473, Reference materials for radionuclides in environmental samples (Second Edition). Vienna, Austria: IAEA.

International Atomic Energy Agency (IAEA). (2022). Technical Reports Series No. 473, Reference materials for radionuclides in environmental samples (Second Edition). Vienna, Austria: IAEA.

International Commission on Radiological Protection (ICRP). (2017). Publication 132: Radiological protection from cosmic radiation in aviation. Annals of the ICRP. 2017;46(3-4):1-139.

Lutz, W., & Samir, K. (2017). World population dynamics: Demographic trends in a complex world. World Scientific.

Majeed, A. A., & Abu-Khader, M. M. (2014). Determination of natural radioactivity in environmental samples using high resolution gamma-ray spectroscopy. Journal of Radioanalytical and Nuclear Chemistry, 299(1), 49-57.

McNeill, J. R. (2000). Something New Under the Sun: An Environmental History of the Twentieth Century. W.W. Norton & Company.

Mohammad, W. Kadi & Dheyab, A. Al-Eryani. (2012). Natural Radioactivity and Radon Exhalation in Phosphate Fertilizers. Arabian Journal for Science and Engineering volume 37, pages225–231.

Nada, A., Abd-ElMaksoud, T.M., Abu-Zeid, H.M., El-Nagar, T. & Awad, S. (2009). Distribution of radionuclides in soil samples from a petrified wood forest in El-Qattamia, Cairo, Egypt. Appl. Radiat. Isot. 67, 643.

National Council on Radiation Protection and Measurements (NCRP). (2014). Report No. 164: Evaluation of screening models used for assessing the radiological impact of uranium mining and milling operations. Bethesda, MD, USA: NCRP; 2014.
National Council on Radiation Protection and Measurements (NCRP). (2009). Recommendations on limits for exposure to ionizing radiation. NCRP Report No. 160. Bethesda, MD: NCRP.
National Council on Radiation Protection and Measurements (NCRP). (2014). Report No. 164: Evaluation of screening models used for assessing the radiological impact of uranium mining and milling operations. Bethesda, MD, USA: NCRP; 2014.
UNSCEAR (2008). Sources and Effects of Ionizing Radiation. United Nation Scientific Committee on the Effects of Atomic Radiation Sources to the General Assembly with Annexes, Report to the General Assembly, with Scientific Annexes, New York: United Nations Publication.
UNSCEAR (2000). United Nations Scientific Committee on the Effects of Atomic Radiation. Sources and Effects of Ionizing Radiation (Volume I). New York: United Nations.
United Nations Environment Programme (UNEP). (2019). Global Environment Outlook 7. Synthesis Report. Nairobi, Kenya: UNEP.
World Health Organization (WHO). (2021). WHO handbook on indoor radon: A public health perspective. Geneva, Switzerland: WHO.
World Nuclear Association (WNA). (2022). World Uranium Mining. London, UK: WNA.
Worster, D. (1994). Nature's Economy: A History of Ecological Ideas. Cambridge University Press.
Yanagisawa, K. Muramatsu Y. & Kamada, H. (1992). "Tracer Experiments on the Transfer of Technetium from soil to Rice and Wheat Plants," Radioisotopes, Vol. 41, pp. 397-402.